



SMART $Ti_{(50-x)}Al_xNi_{30}Cu_{20}$ ($x = 1, 3, 6$) REINFORCED WITH COHERENT LOW-MISFIT NANOSCALE PRECIPITATES COMPOSITES

Mariana Lucaci¹, Mihaela Valeanu², Delia Patroi³, Diana Cirstea⁴, Sorina Mitrea⁵

¹ INCDIE ICPE-CA, Bucharest, ROMANIA, lucaci@icpe-ca.ro

² INCDFM, Bucharest-Magurele, ROMANIA, valeanu@incdfm.ro

^{3,4,5} INCDIE ICPE-CA, Bucharest, ROMANIA, patroidelia@icpe-ca.ro; dic@icpe-ca.ro, mitrea@icpe-ca.ro

Abstract: The paper presents our research results regarding obtaining of $Ti_{(50-x)}Al_xNi_{30}Cu_{20}$ ($x = 1, 3, 6$) alloys reinforced with coherent low-misfit nanoscale precipitates using spark plasma sintering (SPS). This technique allow obtaining of materials with save of energy and time. The materials exhibit good properties for applications such as self-expanding stents, automotive actuators and other applications wherein shape memory alloys with high output force and long cyclic life are desired.

Keywords: Cu and Al alloyed NiTi shape memory alloys, spark plasma sintering, XRD, martensitic transformation, dispersion strengthening

1. INTRODUCTION

The NiTi alloy has attracted much interest for its potential application in various engineering and medical application areas [1, 2, 3]. It is the most common used as shape memory alloy (SMA). SMA are materials that have two or sometimes several crystallographic phases for which reversible transformations from one to other occur through diffusion-less transformations, the so-called " reversible martensitic transformations" [4]. Two significant effects are related with the phase change: the shape memory effect and the superelasticity. The superelasticity occurs when the martensitic phase transformation is stress induced at a constant temperature. The transformation is characterized by a plateau and a hysteresis upon unloading. The magnitude of reversible "pseudo-elastic strain" can be as high as 8 % or even more for single crystals. The shape memory effect (SME) refers to the ability of the material, initially deformed in its low-temperature phase (called "martensitic"), to recover its original shape upon heating to its temperature phase (called "austenitic or parent phase").

A representation of the shape memory effects is presented in the Fig. 1.

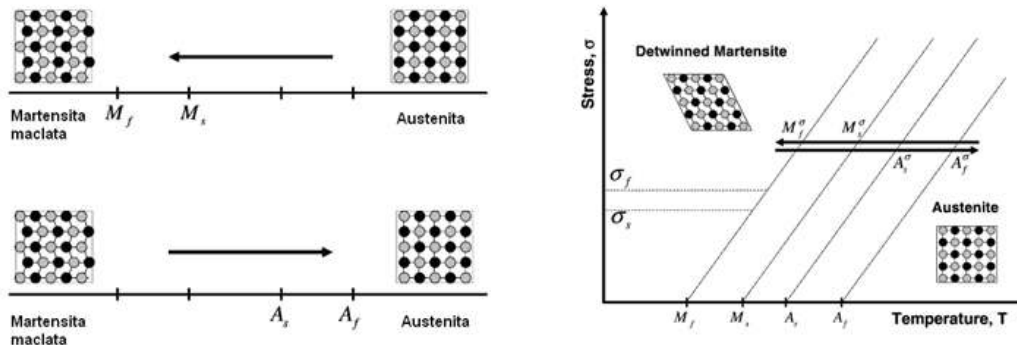


Figure 1. The shape memory effect schematic representation

Based on these effects, the shape memory alloys have to be considered as actuating materials. Over the last decade, micro-grippers, micro-valves and micro-pumps, spacers and a lot of medical pieces, have been reported.

[5]. It is known that processing of Ni-Ti base SMAs materials requires special attention. Usually these materials are made by melting processes which are associated with a slight contamination of material due to the high reactivity of the melt. The poor workability and other problems associated with casting, such as segregation of alloying elements and excessive grain growth, enhance the interest in powder metallurgical (PM) and Mechanical Alloying (MA) as an alternative to prepare the alloy.

The addition of the third alloy elements (Fe, Cu, Nb, Hf, etc.) allows modifying the phase transition temperature and thus the functional properties of these alloys. For example Ni-Ti-Cu SMAs show a narrow hysteresis and a moderate dependence of phase transition temperatures on alloy composition [6], while Ni-Ti-Hf alloys exhibits relatively high phase transition temperature [7].

By adding Al, Zr, Pd and Pt into NiTi alloy, the strengthening of the parent phase is produced and thus, the output force and cyclic lifetime of the NiTi alloys is improved [8]. Addition of such additives produces less than about 2.5 % misfit in the lattice parameter without causing irreversible effects on the martensitic transformation. Lattice misfit arising from different lattice parameters between two coherent phases causes coherency strains with an associated volume strain energy that act as obstacles to martensite interfacial motion, potentially increasing the transformation hysteresis (Af-Ms).

In this paper are reported the results obtained on the synthesized $Ti_{(50-x)}Al_xNi_{30}Cu_{20}$ ($x = 1, 3, 6$) alloys starting from elemental powders, using spark plasma sintering.

2. EXPERIMENTAL PROCEDURES

Commercially Ni, Ti, Cu and Al elemental powders were used to obtain the $Ti_{(50-x)}Al_xNi_{30}Cu_{20}$ ($x = 1, 3, 6$) alloys. The samples were codified as C1, C2 and C3 respectively. The elemental powders were weighed at the desired composition, mixed together in order to obtain a homogenized mixture and then were introduced in a cylindrical graphite die having 40 mm in diameter, in order to be SPS processed. The SPS process was done in argon atmosphere, at the 850 °C temperature under a pressure of 36 MPa. A single pulse was applied. The SPS cycle is presented in the Fig.2.

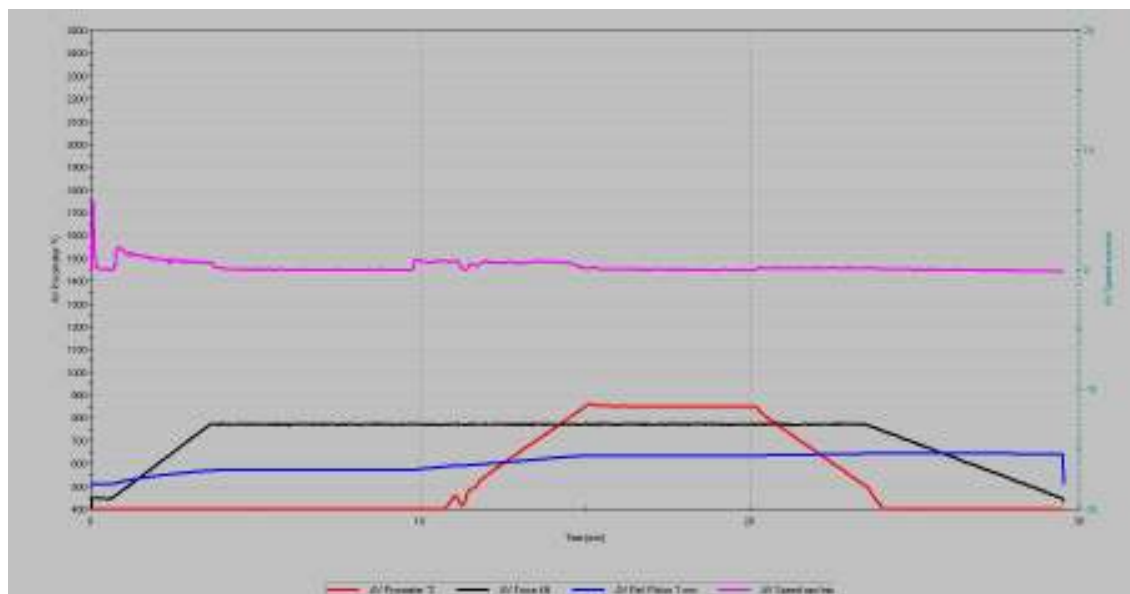


Figure 2. The SPS used process parameters

For each composition it was obtained a cylindrical sample which was annealed at 600 °C for 72 hours in argon atmosphere. Cooling of samples was done under argon atmosphere with a cooling rate of 5°C/min. The materials were finally aged at 450 °C for 4 hours in evacuated quartz capsule followed by quenching into oil. The X-ray diffraction was carried out using a Siefert Diffractometer with Cu anode with wave length of 5405 Å and Ni crystal monochromator. The hardness of the materials was determined using a FM 700 Vickers, XMO 195 series microhardness tester. The testing was done at the force of 0.3kgf for test duration of 15 seconds. In order to detect the temperature transformation a TG-DSC/DTA thermal instrument was used. The DSC analysis was performed under argon atmosphere and the heating/cooling rate was of 10 K/min.

3. RESULTS AND DISCUSSIONS

3.1. Porosity and density

Pores are inevitable components of the microstructure when sintering is applied. Their diameter mainly depends on particle size and sintering condition.

The density of compacts was calculated from the ratio of volume (V) and mass (m) which was reported to the theoretical density calculated with the formula:

$$\frac{1}{\rho_{\text{alloy}}} = \sum_{i=1}^n \frac{f_i}{\rho_i} \quad (1)$$

In which ρ_{alloy} is the density of the synthesized material, i = number of components, f_i = fraction of component i and ρ_i = density of component i .

The calculated density of the materials was 6.2, 6.17 and 6.11 g/cm³ for C1, C2 and C3 material respectively. The synthesized density materials calculated from the ratio of volume and mass was of 6.015, 6.006 and 6.02 g/cm³ for C1, C2 and C3 material respectively. It can be observed that the materials density does not depend on the amount of Al contents. This behavior is closely related to decrease of the porosity due to the fact that at the sintering temperature the aluminum becomes liquid producing contraction phenomena together with forming of new phases having other molar volume and crystal lattice parameters.

The total porosity (P_T) was calculated as an empty volume from the density as follows:

$$P_T = \left(1 - \frac{\rho_{\text{alloy}}}{\rho_T}\right) \cdot 100, \% \quad (2)$$

where: ρ_{alloy} is the measured density of the materials and ρ_T – theoretical density for the studied materials

With increasing of Al content the fraction of pore volume decreases as shown in Figure 3.

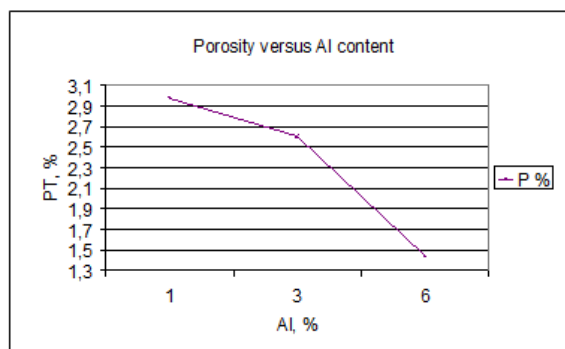


Figure 3. Variation of the porosity as a function of Al contents

3.2. The materials microhardness

The microhardness obtained values are in close relation with the new formed phases during the synthesis of the materials. (Table 1).

Table 1. The hardness obtained values of the synthesized materials

Material type	Al at%	HV 0.3/15 average value
C1	1	548.6
C2	3	529.8
C3	6	591.8

While it was expected that the hardness of the material to increase with the aluminum content, these values are not strongly related with the amount of aluminum in the synthesized materials. At 3 at % Al, the C2 material presents the lowest value of the microhardness, value that can be explained by the fact that this material is constituted from many phases having different values of the microhardness. This fact can be proved by the shape

of the indentation. The imprint on this material has a varied border, due to the fact that this material is constituted from many phases. Nevertheless, the microhardness values are nearest as magnitude.

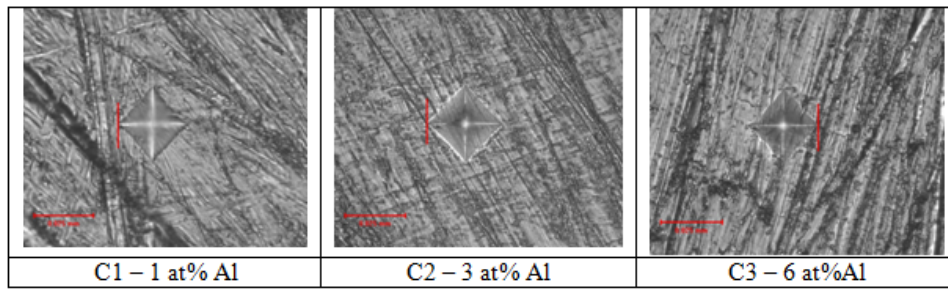


Figure 4. The shape of HV indentation of the materials

3.3. The X-ray diffraction results

As shown in the figure 5, all type of materials is constituted from a B2 type NiTi mainly phase and secondary phases, which comprise Ni_2Ti intermetallic compounds. At room temperature the materials are in austenitic state result which is in concordance with those reported by Jin –Won Jung [8].

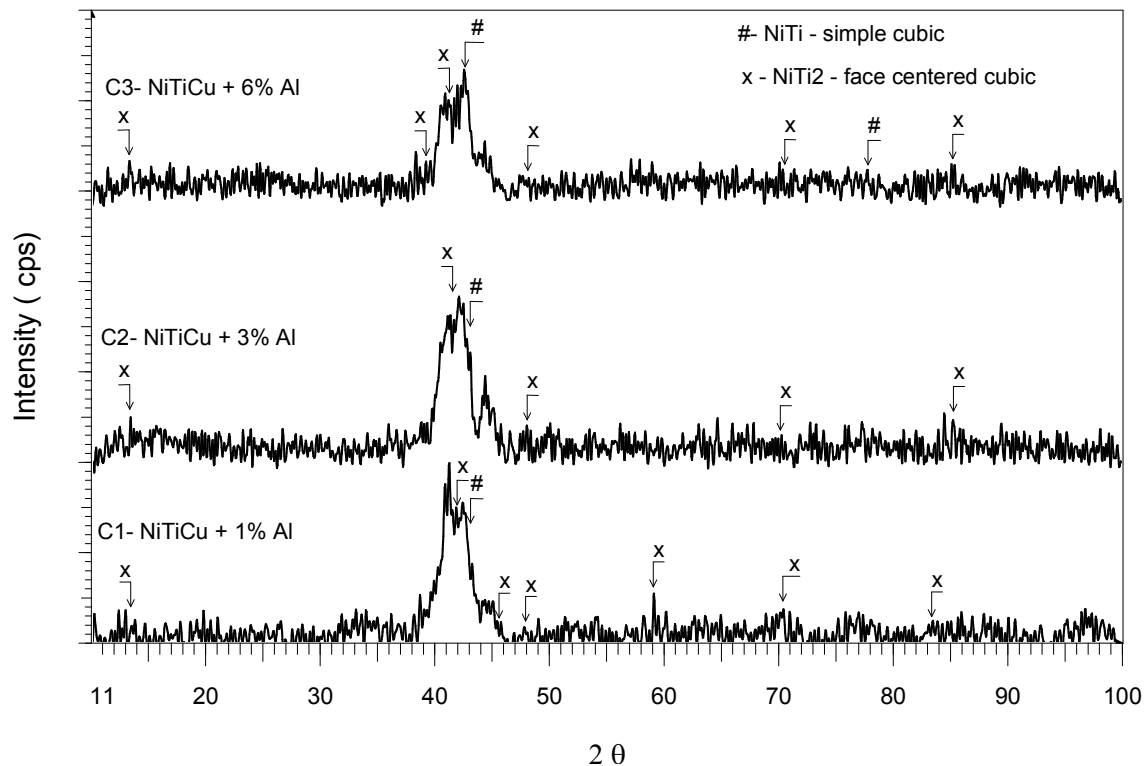


Figure 5. The experimental XRD pattern of the synthesized materials

The experimental lattice parameters for all indexed phases (table 2) showed that these phases have an expanded lattice parameters caused by the presence of the alloying elements Cu and Al. Cu as substitute for Ni in the NiTi phase produces a dilatation of the crystalline lattice because of its atomic radius higher than Ni.

The Ti_2Ni phase act as reinforcer for the parent phase (B2) of the matrix. This strengthening is necessary to improve the output force and the cyclic lifetime of SMAs. By raising the critical shear stress for slip, the irreversible slip deformation during the martensite reorientation and stress induced martensite transformation can be suppressed which, in turn, improves the shape memory effect and transformation superelasticity characteristics.

Table 2. The lattice parameters and the average size crystallite of the observed phases

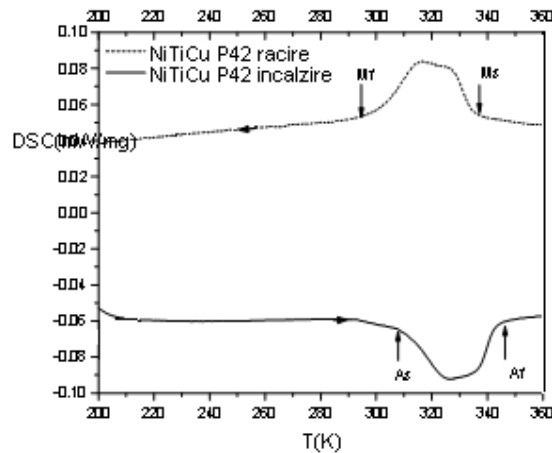
Sample	PHASE	(h,k,l) planes	Crystallization system	a=b=c, Å (PDF pattern)	a=b=c, Å (experimental)	D (nm)
C1	NiTi ₂	(5,1,1)	fcc	11,3193	11,3209	25,9
	NiTi	(1,1,0)	B2	2,998	3,004	26,0
C2	NiTi ₂	(5,1,1)	fcc	11,3193	11,3656	22,7
	NiTi	(1,1,0)	B2	2,998	3,012	26,0
C3	NiTi ₂	(5,1,1)	fcc	11,3193	11,344	25,9
	NiTi	(1,1,0)	B2	2,998	3,007	26,0

The average sizes of the crystallite are very close one with other and this value is close to 26 nm. Al alloying element has significant solubility in the B2 matrix, and has as main effect, drastically decreasing of the transformation temperatures.

3.4. Temperature transformation results

The temperatures transformation of the Cu and Al alloyed NiTi materials were to low in order to be detected by the used DSC equipment, as [8] have showed.

The temperature transformation of the sintered NiTiCu materials used as reference material is shown in the figure 6.

**Figure 6 .** The heating and cooling DSC curves

The both, martensitic and austenitic transformation seems to be the results of two simultaneous transformations which take place in the material at the characteristic temperatures painted in the table 3.

Table 3 The characteristic temperatures of the phases transformation obtained from DSC analysis

P42 NiTiCu	Ms[K]	Mf[K]	As[K]	Af[K]
	337	294	307	345

In order to detect the characteristic temperature values for the Ni-Ti-Cu-Al materials is required to use performed DSC equipment or to use some alloying elements which can act as martensite stabilizer, in order to increase the temperature transformation. In opinion of Jin-Won Jung [8], these stabilizers can be chosen from the group of the element having the role in reducing the interface lattice misfit between the B2 matrix and the hardening phases containing aluminum (Ni₂TiAl), such us Hf, Zr, Pd and Pt.

3. CONCLUSION

The Ni-Ti-Cu-Al alloys have been manufactured using a spark plasma sintering equipment. The results obtained are as follows:

Adding of Al in Ni-Ti-Cu materials have been made with the aim to increase the out put force and the lifecycle of the materials.

Al alloying element for Ni-Ti-Cu materials produce a strong decrease of the transformation temperatures.

Addition of martensite stabilizers are needed to increase the transformation temperature values.

ACKNOWLEDGEMENTS

The work was performed under the Romanian National Research Programme within the 71-116 project.

REFERENCES

- [1]. J. Frenzel, J. Pfetzing, K. Neuking, G. Eggeler, Mater. On the influence of thermomechanical treatments on the microstructure and phase formation behaviour of Ni-Ti-Fe shape memory alloys, *Sci.Eng. A* (2007), doi: 10.1016/j.msea.2007.03.115.
- [2]. Ming H. Wu, Fabrication of Nitinol materials and components, *Proc. Of International Conference on Shape Memory and Superelastic Technologies*, Kunming, China, p 285-292, (2001)
- [3]. M.C.A. da Silva et al, Microstructural characterization of equiatomic NiTi alloy prepared by high energy milling, *Mat. Sci. Forum*, Vols. 530-531, p 53-58, (2006).
- [4]. L. Delay, in: R.W. Cahn, P. Haasen, E.J. Kramer (Eds.), *Mater. Sci. Technol.*, vol. 5, "Phase transformations in Materials" VCH, Weinheim, (1991)
- [5]. Y. Bellouard, *Mater.Sci. Eng. A.* (2007), doi: 10.1016/j.msea.2007.02.166
- [6]. Y. X Tong et al, Characterization of a nanocrystalline NiTiHf high temperature shape memory thin film, *Scripta Mater.* 52, p 983-987, (2005)
- [7]. T. H. Nam, T Saburi, K. Shimizu, *Mater.*, Cu content dependence of the shape memory characteristics in the NiTiCu alloys, *Trans., JIM* 31 p 959, (1990)
- [8]. Jin-Won Jung, Gregory B. Olson, Coherent nanodispersion-strengthened shape memory alloys, US Patent 0187980 92004)